

Imaging material properties by resonant tapping-force microscopy: A model investigation

R. G. Winkler*

Abteilung Theoretische Physik, Universität Ulm, 89069 Ulm, Germany

J. P. Spatz, S. Sheiko, and M. Möller

Organische Chemie III—Makromolekulare Chemie, Universität Ulm, 89069 Ulm, Germany

P. Reineker

Abteilung Theoretische Physik, Universität Ulm, 89069 Ulm, Germany

O. Marti

Experimentelle Physik, Universität Ulm, 89069 Ulm, Germany

(Received 27 February 1996)

The interaction of a cantilever performing a forced oscillation with a sample in a tapping-mode scanning force microscope is investigated within a simple model. The tip together with the cantilever is modeled as a periodically driven, damped harmonic oscillator. The viscoelastic sample is described by a friction force acting on the tip while it is in contact and a harmonic potential. The penetration of the probe and the phase shift of the oscillator due to contact with the sample are calculated for various sample parameters. In particular, an approximate solution of the model equations for the phase shift is presented. Moreover, a relation between the elastic constant of the model and the elastic modulus of a material is presented. [S0163-1829(96)04136-7]

I. INTRODUCTION

Scanning force microscopy (SFM) has evolved to the most powerful surface analyzing tool over the last few years. Many subfields developed, driven by the potential to image surfaces with various physical properties down to molecular and atomic resolution.^{1,2} Various operating principles of SFM were designed in order to reduce surface destruction and to image soft surfaces such as polymers and biological samples. Among these the so-called tapping-mode force microscope minimizes surface contacts and lateral forces by periodically touching the surface with the cantilever.³

In a tapping-mode force microscope, the tip is externally driven with a frequency close to the resonance frequency of the oscillation in air. This frequency is high enough to touch a surface area comparable to the tip contact area several times before moving the tip laterally. Moreover, the energy of the cantilever-tip system is large enough to avoid sticking of the tip to the surface. The vibrational amplitude assumes values between 30 and 100 nm. The contact with the surface reduces the amplitude. Usually, the tapping-mode force microscope is operated in a constant amplitude mode, i.e., the amplitude is reduced until a feedback set point is reached. The tapping-mode force microscope has successfully been applied to investigate soft samples.³⁻⁷ The deflection and harmonic resonance frequency of commercial V-shaped and rectangular atomic force microscope cantilevers have been determined experimentally and theoretically by several authors.⁸

Recently tapping-mode force microscopes were developed which aside from the amplitude changes simultaneously detect the phase shift between the free oscillation in air and the oscillation while the tip is touching the surface during a period. As far as structural properties of a surface

are concerned, the phase shift yields information comparably to the changes in the amplitude.

The SFM images reflect the mechanical properties of the sample averaged over the tip contact area.⁹ Thus the SFM not only allows one to detect structural features of a surface but also the mechanical properties of a sample on a nanometer scale. To extract the elastic constants from an image requires a model which connects the measured changes in the amplitude and/or the phase with the desired sample parameters.

In this paper we present a simple model calculation for the interaction of a cantilever performing a forced oscillation with a sample surface. The tip together with the cantilever is modeled as a periodically driven, damped harmonic oscillator. The viscoelastic sample is described by a friction force acting on the tip while it is in contact and a harmonic potential (elastic part). The penetration of the sample, forces, and phase shifts of the oscillator due to contact with the sample are calculated for various sample parameters. The model calculations are extensions of our previous investigations on the influence of forces on the sample in tapping mode.¹⁰

The paper is organized as follows: in Sec. II the model is presented and the results are described in Sec. III.

II. MODEL OF THE TAPPING MODE

The tapping process during a cycle of the forced oscillation can be decomposed into two parts: (i) the tip is in air and (ii) the tip is in contact with the sample. To keep the model simple, we will assume that the tip only interacts with the surface when it is in contact, i.e., there are no long range attractive forces between the tip and the sample. The tip, which is approximated by a mass point, experiences the following potential (see Fig. 1):

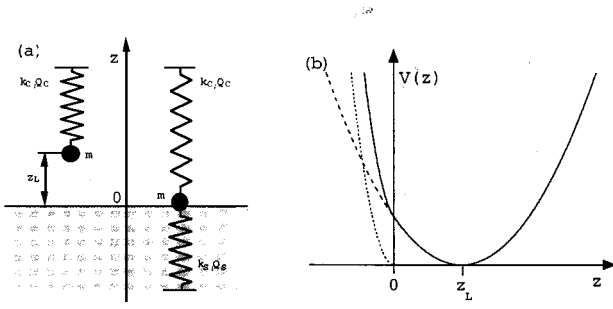


FIG. 1. (a) Model of the forced cantilever oscillation. The cantilever is approximated by a spring with spring constant k_c and quality factor Q_c . z_L is the equilibrium position in air (left side). The inertial part of the cantilever is described as a mass point with mass m . On the right hand side the tip is in contact with the sample characterized by the spring constant k_s and quality factor Q_s . (b) Harmonic potentials experienced by the point mass m . (---) Potential describing the cantilever. (···) Potential of the sample. (—) Total potential of the cantilever-surface system.

$$V(z) = V_s(z) + V_c(z, t), \quad (1)$$

where

$$V_c(z, t) = \frac{k_c}{2} [z - z_L(t)]^2, \quad (2)$$

$$V_s(z) = \frac{k_s}{2} z^2 [1 - \Theta(z)]. \quad (3)$$

The cantilever is described as a harmonic spring with the spring constant k_c and the time dependent equilibrium position $z_L(t)$. Since the cantilever is periodically driven $z_L(t)$ is given by

$$z_L(t) = z_L + a \cos(\omega t). \quad (4)$$

Here $z_L (\geq 0)$ denotes the average position of the driving piezo crystal, ω its frequency, and a its amplitude of oscillation. k_s denotes the spring constant of the sample and Θ is Heaviside's step function.

The equation of motion of the mass m in the potential V [Eq. (1)] is given by

$$\ddot{z}(t) + \{2\gamma_c + 2\gamma_s[1 - \Theta(z)]\}\dot{z}(t) + \omega_c^2[z(t) - z_L] + \omega_s^2 z(t)[1 - \Theta(z)] = a\omega_c^2 \cos(\omega t). \quad (5)$$

Aside from the elastic forces, this equation includes the damping of the cantilever $2\gamma_c = \omega_c/Q_c$, where ω_c is the eigenfrequency of the cantilever and Q_c its quality factor. The viscous part of the sample is taken into account by the friction force $2\gamma_s \dot{z}(t)[1 - \Theta(z)]$. The friction constant can also be related to the eigenfrequency of the sample ω_s and its quality factor Q_s via $2\gamma_s = \omega_s/Q_s$. The eigenfrequencies themselves depend on the spring constants via

$$\omega_c = \sqrt{\frac{k_c}{m}}, \quad \omega_s = \sqrt{\frac{k_s}{m}}. \quad (6)$$

Due to the presence of the Θ function, Eq. (5) is nonlinear and an analytical solution (for all times) cannot simply be given. However, during the time interval in which the tip is

in air or in the sample within a period of oscillation, respectively, we obtain two linear equations of motion with parameters characterizing the cantilever or the combination of cantilever and sample, respectively. The solution of these equations is given by

$$z(t) = \begin{cases} z_c(t), & z \geq 0 \\ z_{cs}(t), & z < 0 \end{cases} \quad (7)$$

where

$$z_c(t) = e^{-\gamma_c t} [a_c \cos(\omega_c^e t) + b_c \sin(\omega_c^e t)] + A_c \cos(\omega t - \alpha_c) + z_L, \quad (8)$$

$$z_{cs}(t) = e^{-\gamma_{cs} t} [a_{cs} \cos(\omega_{cs}^e t) + b_{cs} \sin(\omega_{cs}^e t)] + A_{cs} \cos(\omega t - \alpha_{cs}) + \tilde{z}_L. \quad (9)$$

The parameters of the combination of cantilever and sample are $\omega_{cs}^2 = \omega_c^2 + \omega_s^2$ and $\gamma_{cs} = \gamma_c + \gamma_s$. The A_i ($i = c, cs$) denote the amplitudes of the particular solutions of Eq. (5) given by

$$A_i = \frac{a\omega_c^2}{\sqrt{(\omega_i^2 - \omega^2)^2 + 4\gamma_i^2 \omega^2}}. \quad (10)$$

α_i denotes the phase shifts

$$\tan \alpha_i = \frac{2\gamma_i \omega}{\omega_i^2 - \omega^2}. \quad (11)$$

Finally, ω_i^e is the eigenfrequency of the damped system

$$\omega_i^e = \sqrt{\omega_i^2 - \gamma_i^2}, \quad (12)$$

and

$$\tilde{z}_L = \frac{\omega_c^2}{\omega_{cs}^2} z_L \quad (13)$$

the equilibrium position of the cantilever-sample system. The two solutions Eqs. (8) and (9) need to be combined in such a manner that z and \dot{z} are continuous whenever the tip touches or leaves the surface. Together with the initial condition these requirements determine the four coefficients a_i and b_i . Since our original differential equation (5) is nonlinear, the coefficients a_i and b_i depend on time.

As pointed out earlier, the total potential (1) is nonlinear due to the presence of the Θ function. This nonlinearity may result in a chaotic behavior of the tip for certain model parameters. However, we did not observe any trace of chaos for the parameters used in our calculations.

Additionally, in real materials the interaction of the tip with the substrate is nonlinear, which we describe in the present paper by a harmonic potential. This is certainly a crude approximation and is only used due to the lack of an appropriate description of the tip-surface interaction, especially for soft samples. A Lennard-Jones type potential may adequately be used for solid samples. However, for organic substances other potentials should be more appropriate. The harmonic potential just serves as a first approximation to investigate the principle mechanisms in the tip-surface interaction of a tapping-force microscope.

To compare our analytical solution with experimental results, we chose the parameters according to values used in experiments. In detail, the tapping frequency ω is set equal to the resonance frequency $\omega = \omega_r = 2\pi 340.575$ kHz of the cantilever in air and the spring constant $k_c = 50$ N/m. The amplitude a of the piezo oscillations and the quality Q_c of the cantilever are extracted from the resonance curve of the cantilever in air. From the comparison of the half-width at half maximum of the experimental resonance curve and the theoretical one we find $a \approx 0.0269$ nm and $Q_c \approx 700$.

The tapping-mode scanning force microscope is operated in a constant amplitude mode. Via a feedback loop the height (z_L) of the piezo-cantilever system is adjusted such that the amplitude of the oscillations, with the cantilever touching the surface, assumes a set value (set point a_{set}). In a similar manner we determined the solution of our model system. We chose the set point $a_{\text{set}} = 0.65a_m$, where $a_m = 18.84$ nm is the maximum of the resonance curve of a cantilever in air. The height z_L of the equilibrium position of the externally driving force is now adjusted until the stationary solution assumes the set-point amplitude. From that stationary solution we extract the penetration of the sample and the phase shift of the oscillation with respect to the one of the driving force.

III. RESULTS

The solution $z(t)$ [Eq. (7)] assumes a stationary state after an equilibration time. The oscillation is then periodic but not necessarily harmonic, especially for strong tip-surface interactions. The time for the equilibration naturally depends on the tip-surface interaction parameters.

Two quantities can be extracted from the model calculations, which ultimately depend upon the sample properties: (i) the height z_L of the equilibrium position of the cantilever-piezo system and (ii) the phase shift of the forced oscillation.

To determine the equilibrium position z_L , we adjusted the height z_L in such a way that the deformation of the sample (z_{def}) plus z_L are equal to the set-point amplitude ($a_{\text{set}} = z_L + z_{\text{def}}$) by a feedback loop. The sample deformation itself is given by the minimum value of $z(t)$ in the stationary state [$z_{\text{def}} = |\min z(t)|$]. In our calculations the set point is obtained with an accuracy $|(z_L + z_{\text{def}})|/a_{\text{set}} < 10^{-9}$ for all parameters used.

Figure 2 shows the dependence of the sample deformation on its stiffness k_s for various sample damping constants (γ_s). (Notice the log-log representation.) The damping constants used in the figure are $2\gamma_s = 10^{-3+n/3}\omega_c$, where $n = 0, 1, \dots, 18$. Obviously, the deformation decreases with increasing stiffness and damping of the sample. There are remarkably large ranges of sample stiffnesses, where the sample deformation is independent of k_s . This range is increasing with increasing sample damping. For all damping constants γ_s the curves of the sample deformation approach a limiting curve which decreases with increasing sample stiffness as $z_{\text{def}} \sim k_s^{-2/3}$. As a consequence, within the plateau regions, samples with the same damping constant but different stiffnesses cannot be distinguished by tapping scanning force microscopy. Scans of such samples produce the same image and erroneously indicate similar material properties, although the elasticity constants may differ by several decades. On the other hand, a quantitative comparison of vari-

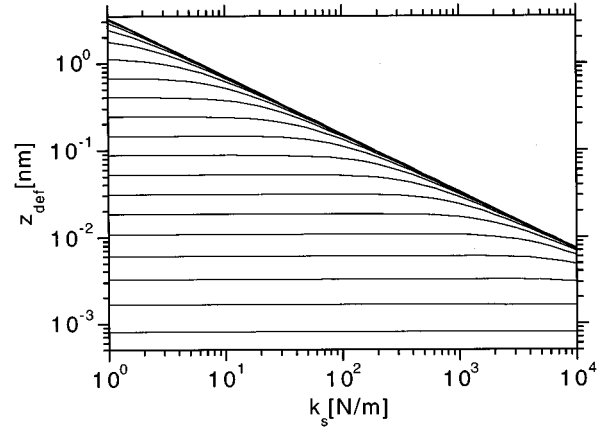


FIG. 2. Deformation z_{def} of the sample versus sample stiffness k_s for various sample damping constants γ_s in a log-log representation. The damping constants are $2\gamma_s = 10^{-3+n/3}\omega_c$, where $n = 0, 1, \dots, 18$ and ω_c is the frequency of the cantilever. The damping constant increases from top to bottom. All curves approach the limiting curve $z_{\text{def}} \sim k_s^{-2/3}$ for sufficiently large k_s . The equilibrium position z_L of the cantilever-tip system is obtained from the sample deformation by the relation $z_L = a_{\text{set}} - z_{\text{def}}$.

ous materials is practically only possible within the parameter values where the deformation is changing according to the power law $z_{\text{def}} \sim k_s^{-2/3}$. Otherwise the detailed dependence of the deformation on the sample parameters has to be known. As mentioned before, the limiting curve is approached for all damping constants. Thus for sufficiently large k_s or small γ_s , respectively, the elastic constants can be determined independently of the damping of the material.

Material properties can also be extracted from the phase shift between the driving oscillation and the stationary oscillation $z(t)$ [Eq. (7)]. We determine the phase shift between the two oscillations whenever the mass point (tip) approaches the surface and is at z_L . The phase shift is then given by $\sin\alpha = -\cos(\omega t)$ or, if $\sin\omega t < 0$, by $\alpha = \pi/2 + |\alpha - \pi/2|$, where t is the time at which $z(t) = z_L$. The dependence of the phase shift on sample stiffness and sample damping is shown in Fig. 3 (γ_s increases from bottom to top). As is obvious from the plot, all curves approach two limiting curves and decrease monotonously with increasing sample stiffness. In the limit $k_s \rightarrow 0$ the curve for infinite sample damping (top line) is approached and in the limit $k_s \rightarrow \infty$ the curve for zero sample damping (bottom line) is approached. Similarly to the sample deformation the phase shift approaches constant values. But the constants are assumed for small and large damping. In these regimes no distinction is possible between materials of different sample stiffnesses. Despite this, from the phase shift material properties can be extracted for sample stiffnesses where the sample deformation is constant. By comparing Figs. 2 and 3, we observe variations in α for k_s values where the sample deformation is constant, especially for $\gamma_s \approx 1 - 10$. Hence phase shift images may yield a small contrast even though deformation images show none.

The phase shift depends nonlinearly on the material properties. Thus for a quantitative comparison between different images the knowledge of this functional dependence is required, i.e., material properties can only be extracted from

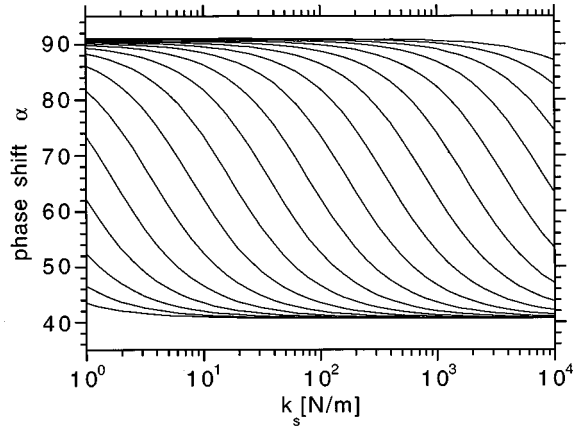


FIG. 3. Phase shift α between the piezo oscillation and the oscillation of the cantilever touching the sample during one period versus the sample stiffness k_s for various sample damping constants γ_s . The damping constants are $2\gamma_s = 10^{-3+n/3}\omega_c$, where $n=0,1,\dots,18$ and ω_c is the frequency of the cantilever. The damping constant increases from bottom to top.

images if a suitable model calculation yields a relation between the measured phase shift and the material parameters. Although our calculations are based on harmonic potentials, the combination of the two potentials makes the problem highly nonlinear. Thus an exact analytical solution beyond Eqs. (7)–(9) cannot be given. However, an approximate expression of the phase shift is obtained in the following way. In the stationary state the solution $z(t)$ is periodic but not necessarily harmonic. We approximate the stationary solution by the harmonic expression

$$z_{\text{app}}(t) = B \cos(\omega t - \alpha). \quad (14)$$

The effective frequency and damping constant are assumed to be a linear combination of the frequencies and the damping constants of the cantilever and the sample,

$$\omega_e^2 = \omega_c^2 + \beta \omega_s^2, \quad (15)$$

$$\gamma_e = \gamma_c + \beta \gamma_s. \quad (16)$$

Moreover, we assume that the amplitude B and the phase shift α depend on the effective parameters in the same way as the amplitudes A_i of Eq. (10) and the phase shifts of Eq. (11), i.e.,

$$B = \frac{a \omega_c^2}{\sqrt{(\omega_e^2 - \omega^2)^2 + 4 \gamma_e^2 \omega^2}}, \quad (17)$$

$$\tan \alpha = \frac{2 \gamma_e \omega}{\omega_e^2 - \omega^2}. \quad (18)$$

Since we operate the tapping-force microscope in a constant amplitude mode, we can extract the coefficient β from Eq. (17) and use this value to calculate the phase shift. Equation (17) can simply be solved, because β is included in quadratic form. The comparison between the exact solution for the phase shift and the analytical approximation exhibits excellent qualitative agreement. Quantitative agreement is only obtained for small damping constants and set points close to

the maximum amplitude in air. For the parameters tested, we find quantitative differences up to 10%.

The maximum force exerted on the sample by the tip is given by the linear relation

$$F = k_s z_{\text{def}}. \quad (19)$$

Thus the force is linearly increasing for increasing sample stiffnesses where z_{def} is constant and increases as $k_s^{1/3}$ when $z_{\text{def}} \sim k_s^{-2/3}$. As discussed in Ref. 10, the force experienced by the sample strongly depends on the tapping frequency. A detailed discussion of the frequency dependence of the force in a constant amplitude mode will be given elsewhere.

Using the Hertz model,^{4,11,12} the sample stiffness can be related to elastic moduli of the sample. Thus material properties can be extracted from tapping-mode measurements. For the special case of one sphere of radius R and the second sphere of infinite radius (plane) the radius (r) of the contact area between these two smooth elastic bodies under a load F is

$$r = \left(\frac{FR}{E^*} \right)^{1/3}. \quad (20)$$

E^* is related to the elastic moduli of the two materials. The assumption that the Young modulus of the tip is much larger than that of the surface yields the relation

$$E^* = \frac{4}{3} \frac{E}{1 - \nu^2}, \quad (21)$$

where ν and E are the Poisson ratio and the Young modulus of the surface, respectively. Due to the load, the sphere penetrates into the surface a distance h which is related to the force by

$$F = \sqrt{RE^*} h^{3/2}. \quad (22)$$

The stiffness of the sample follows from Eq. (22) as derivative with respect to h and is related to the spring constant by

$$k_s = \frac{3}{2} E^* \sqrt{Rh} = \frac{3}{2} E^* \sqrt{R z_{\text{def}}}. \quad (23)$$

To obtain the last relation, we used the fact that the penetration h is identical to the deformation z_{def} of our model calculation. Thus the spring constant is proportional to the elastic constant of the material. Since the deformation z_{def} is measured in a tapping-mode force microscope ($z_{\text{def}} = a_{\text{set}} - z_L$) the material constants can be related to the model parameters.

In summary, we have presented a simple model for the interaction of a cantilever performing a forced oscillation with a sample surface in a tapping-mode scanning force microscope. Similarly to a real experiment, we measured the height of the equilibrium position of the cantilever above the surface and the phase shift between the driving oscillation

and the stationary oscillation of the tip-cantilever system in a constant amplitude mode for various sample stiffnesses and damping. For the elastic deformation of the sample we find large regimes, where the deformation is independent of the sample stiffness. With increasing sample damping, these regimes are increasing. A limiting curve $z_{\text{def}} \sim k_s^{-2/3}$ is approached for all damping constants and sufficiently large sample stiffnesses. Moreover, an analytical approximation for the phase shift is derived. Using the Hertz model, a relation between the model parameters and the elastic constants of the sample is derived, which allows one to obtain the elastic constants from tapping-mode measurements.

In all the calculations the sample is considered a viscoelastic continuum. However, for tips of nanometer size and structures of comparable size in the samples the continuum approach is rather crude. Considering these aspects, the extraction of molecular parameters of a sample requires a much more detailed model of the tip-substrate interaction.

ACKNOWLEDGMENTS

This investigation is part of a project of the Sonderforschungsbereich (SFB) 239. The support of the Deutsche Forschungsgemeinschaft is gratefully acknowledged.

* Author to whom correspondence should be addressed.

¹G. Binnig, C. F. Quate, and C. Gerber, *Phys. Rev. Lett.* **56**, 930 (1986).

²P. K. Hansma, V. B. Elings, O. Marti, and C. E. Bracker, *Science* **56**, 209 (1988).

³Q. Zhong, D. Inniss, and V. B. Elings, *Surf. Sci.* **290**, L688 (1993).

⁴M. Radmacher, R. W. Tillmann, and H. E. Gaub, *Biophys. J.* **64**, 735 (1993).

⁵R. Höper, R. K. Workman, D. Chen, D. Sarid, T. Yadav, J. C. Withers, and R. O. Loutfy, *Surf. Sci.* **311**, L731 (1994).

⁶K. Umemura, H. Arakawa, and A. Ikai, *J. Vac. Sci. Technol. B* **12**, 1470 (1994).

⁷T. Shibata-Seki, W. Watanabe, and J. Masai, *J. Vac. Sci. Technol. B* **12**, 1530 (1994).

⁸G. Y. Chen, R. J. Warmack, T. Thundat, and D. P. Allison, *Rev. Sci. Instrum.* **65**, 2532 (1994).

⁹M. Radmacher, R. W. Tillmann, M. Fritz, and H. E. Gaub, *Science* **257**, 1900 (1992).

¹⁰J. P. Spatz, S. Sheiko, M. Möller, R. G. Winkler, P. Reineker, and O. Marti, *Nanotechnology* **6**, 40 (1995).

¹¹L. D. Landau and E. M. Lifschitz, *Theoretical Physics* (Akademie-Verlag, Berlin, 1965), Vol. VII.

¹²J. Israelachvili, *Intermolecular and Surface Forces* (Academic Press, London, 1992).